Polymer Journal (2017) 49, 759–765

www.nature.com/pj

FOCUS REVIEW

Preparation of biobased wrinkled surfaces via lignification-mimetic reactions and drying: a new approach for developing surface wrinkling

Hironori Izawa

A simple and green approach to surface wrinkling via a lignification-mimetic reaction and drying is reviewed. A skin layer is synthesized on a chitosan (CS) film via immersion in a methanol solution containing a phenolic acid (PH) and a subsequent surface reaction with horseradish peroxidase (HRP), mimicking wood lignification. A surface relief with micron-scale wrinkles is formed upon drying as a result of inhomogeneous shrinkage. The wrinkle size of this system is predominately determined by the hardness of the skin layer, and the hardness in turn can be controlled by varying both the molecular structure of the PH and the immersion temperature. The crosslinking structure in the skin is composed of ionic bonding between the CS and an oligophenolic residue generated by the HRP-catalyzed surface reaction on the CS, and the quantity of the ionic bonds determines the skin hardness. Furthermore, the wrinkle direction can be highly controlled by the external stress during drying. Notably, this is a totally biobased system that involves green materials and processes.
Polymer Journal (2017) **49,** 759–765; doi:10.1038/pj.2017.52; published online 13 September 2017

INTRODUCTION

Biomimetic systems that imitate the design principles of nature are key technologies for progressing toward environmentally benign and high-performance materials.[1–5] Although cumulative material innovations have enriched our lives, we still have much to learn from nature regarding material design to meet the needs of current times.[6–11]

Surface wrinkling is a ubiquitous physical process that is responsible for the formation of many intriguing surface architectures that plants and animals display.[12,13] This spontaneous process is the result of uneven changes in surface tissue layers with different mechanical properties.[13,14] Nature-mimetic surface designs have been used for nano/microscopic wrinkled surfaces in optical[15] and electronic devices,[16] surface-enhanced Raman spectroscopy substrates,[17] the realization of tunable wettability[18] and adhesion,[19] and the synthesis of cell culture scaffolds.[20] Although many sophisticated systems have been introduced for the development of surface wrinkling, the basic approach remains the same: the fabrication of a hard thin (skin) layer on a soft elastic substrate via dry processing, including chemical vapor deposition,[21] photocrosslinking,[22] and UV/O_3[23] or plasma[24] oxidation, followed by the precise control of stress on the substrate. The available materials for surface wrinkling are thereby limited. Although wrinkled surfaces made from biopolymers are interesting for biomedical applications, it has been virtually impossible to prepare them using dry processing methods because of the difficulty of forming a skin using the previously reported methods as well as the difficulty of controlling the stresses of materials on brittle biopolymer films.

The formation of fine wrinkles in human skin is closely associated with decrease in the water content of the stratum corneum with aging; that is, fine wrinkles are formed by drying and inhomogeneous shrinkage.[25–27] Despite the fact that related processes are ubiquitous in nature,[13] water evaporation during film consolidation to trigger surface wrinkling has hardly been considered.[28,29] We expected that inducing surface wrinkling by inhomogeneous shrinkage upon drying would be a favorable method for producing biopolymer-based wrinkled surfaces that are applicable for biomaterials because, with such an approach, it is not necessary to apply external stresses to induce surface wrinkling.

The nanostructure of wood cell walls is a robust assembly of three primary biopolymers: cellulose, which is present as semicrystalline elementary fibrils; hemicellulose, which acts to decorate and crosslink elementary fibrils and facilitates interactions between other biopolymers; and lignin, which is a crosslinked macromolecular structure based on phenylpropanoid units that associates closely with hemicellulose and adds strength and rigidity to the cell walls.[30–32] Lignin is produced by a natural process, lignification, in which monolignols (three cinnamyl alcohols: *p*-coumaryl, coniferyl and sinapyl alcohols) diffuse to the hemicellulose gel in the wood cell wall and become polymerized and immobilized on hemicellulose during peroxidase and laccase catalysis to strengthen the cell wall.[33] Lignification can be mimicked by oxidizing phenol derivatives using horseradish peroxidase (HRP).[34] Recently, we developed a novel surface wrinkling system inspired by this process (Figure 1).[35–37] A hard skin layer was synthesized via crosslinking using an HRP-catalyzed surface reaction

Department of Science and Biotechnology, Graduate School of Engineering, Tottori University, Tottori, Japan
Correspondence: Dr H Izawa, Department of Science and Biotechnology, Graduate School of Engineering, Tottori University, 4-101 Koyama-Minami, Tottori 680-8550, Japan.
E-mail: h-izawa@chem.tottori-u.ac.jp
Received 9 June 2017; revised 20 July 2017; accepted 30 July 2017; published online 13 September 2017

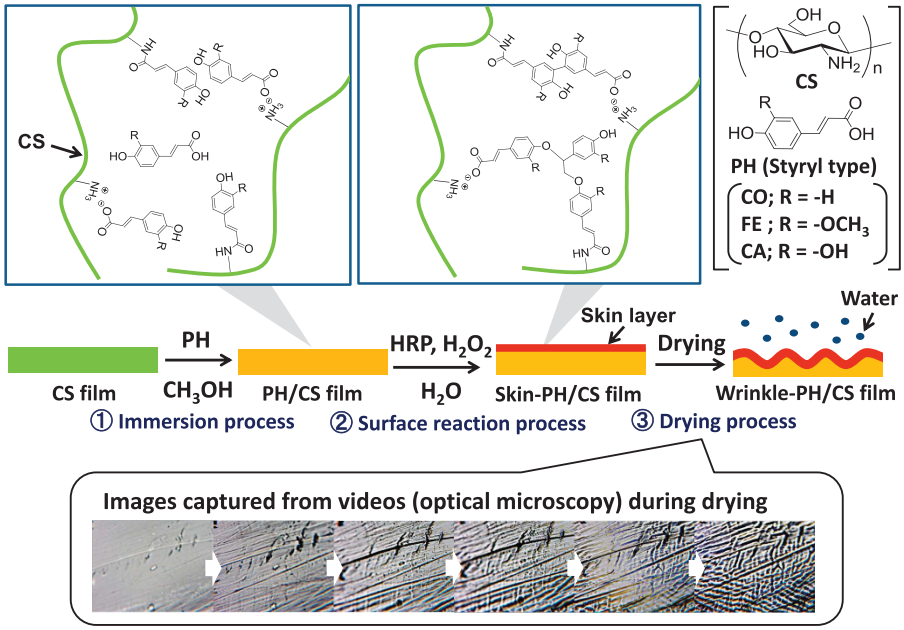

Figure 1 Illustration of the surface wrinkling system introduced in this review. The figure was partially reproduced from Izawa *et al.*[35–37]

of phenolic acid (PH) on a chitosan (CS) film, similar to lignification in wood; that is, the CS film, PH and HRP play the roles of hemicellulose/cellulose, monolignols and oxidases in the wood cell wall, respectively. In addition, surface wrinkling similar to the fine wrinkle formation of human skin was induced by water evaporation. Herein, we overview a biomimetic approach to produce wrinkled surfaces on CS films.

PREPARATION OF WRINKLED FILMS AND CHARACTERIZATION OF THEIR MORPHOLOGIES

Microscopic wrinkles can be fabricated on CS film surfaces using a facile procedure involving immersion, a surface reaction and drying without requiring specialized, electrically powered devices to fabricate the skin layer or to control the material stress. In a typical experiment, a CS film (thickness, ca. 0.1 μm; ϕ, ca. 50 mm) was immersed in methanol (20 ml) containing 0.05 g ml^{-1} PH at 30 °C for 24 h. The resulting film (hereafter, the PH/CS film) was removed and subsequently soaked in water (10 ml), followed by the prompt addition of HRP (1 ml, 137 U) and H_2O_2 (200 μl, 30% concentration). The system was maintained at 30 °C for 12 h, after which the film was removed and dried at 40 °C for 12 h.

Figure 2a–c show plane-view scanning electron microscopy (SEM) images of the surfaces of the wrinkled films obtained using *p*-coumaric acid (CO), ferulic acid (FE) or caffeic acid (CA) − methanol solutions applied for immersion treatment at 30, 40, 50 or 60 °C.[35,36] In all cases, the mean wrinkle wavelengths and amplitudes gradually decreased as the treatment temperature increased. For CO, the mean wrinkle wavelengths and amplitudes after treatment at 30, 40 and 50 °C were 1.53 ± 0.19, 0.90 ± 0.21 and 0.39 ± 0.10 μm, respectively, and 0.30 ± 0.03, 0.23 ± 0.06 and 0.17 ± 0.04 μm, respectively. Interestingly, nanoscale dimples were observed after treatment at 60 °C, which was probably due to the decreased shrinkage stress as described below.[36] The mean dimple wavelength and amplitude were 59 ± 21 and 59 ± 4 nm, respectively. With FE, the wrinkle sizes were similar to those of the CO/CS films; the mean wrinkle wavelength and amplitude after treatment at 30, 40, 50 and 60 °C were 1.82 ± 0.08, 1.28 ± 0.09, 0.72 ± 0.08 and 0.31 ± 0.04 μm, respectively, and 0.43 ± 0.10, 0.46 ± 0.07, 0.25 ± 0.04 and 0.16 ± 0.03 μm, respectively. When CA was used, wrinkling was observed on the wrinkle-CA/CS film using immersion temperatures above 40 °C. Wrinkling did not occur at 30 °C. The mean wrinkle wavelengths and amplitudes after treatment at 40, 50 and 60 °C were much larger (22.4 ± 3.1, 13.3 ± 0.7 or 7.2 ± 0.7 μm, respectively, and 8.2 ± 1.5, 5.8 ± 1.8 or 2.9 ± 0.7 μm, respectively) than those of the FE/CS films.

We also investigated the preparation of wrinkled films using vanillic acid (VA) and homovanillic acid (HO), which are PHs with different substituent groups (R′); however, they all contain a carboxy group (Figure 3a).[37] Figure 3b–c show plane-view SEM images of the surfaces of the wrinkled films prepared after immersion treatment at 30 or 40 °C. For VA, wrinkling occurred after both the 30 and 40 °C immersion treatments. The mean wrinkle wavelengths and amplitudes at 30 and 40 °C were 3.07 ± 0.17 and 1.61 ± 0.25 μm, respectively, and 0.62 ± 0.24 and 0.30 ± 0.10 μm, respectively, which were larger than those of the FE/CS system. When HO was used, wrinkling was observed on the wrinkled HO/CS film at an immersion temperature of 40 °C. The mean wrinkle wavelength and amplitude values under immersion treatment at 40 °C were 2.96 ± 0.16 μm and 0.68 ± 0.18 μm, respectively, which were larger than those for the VA/CS system at 40 °C. Wrinkling did not occur at 30 °C. The same phenomenon was observed in the CA/CS system.

MECHANISM OF SKIN LAYER FORMATION

The absence of wrinkling after the immersion treatment at 30 °C using CA or HO clearly indicated that the immersion process played a crucial role in the wrinkling. Nuclear magnetic resonance, infrared and elemental analyses of the PH/CS films after washing using Soxhlet extraction revealed the formation of covalently bound PH on the CS film via an amide bond, which was facilitated by the simple immersion of the CS film in the PH–methanol solution.[35,37] The dehydration condensation reaction between primary amines and carboxylic acid under the mild immersion conditions was unexpected because such a reaction generally occurs at high temperatures in the presence of

strong acid in a nonpolar solvent.[38] However, it is possible that amides were formed at the CS interface through ester exchange reactions since a small amount of the methyl ester of PH was generated by virtue of the presence of a large amount of methanol. In light of this, we proposed that the dehydration condensation reaction occurred between CS and PH during the immersion process. The covalently bound PH worked as a reaction site on the CS film for the HRP-catalyzed surface reaction and formed a skin layer, as shown in Figure 4. Thus, we concluded that the absence of wrinkling on the CA/CS and HO/CS systems was due to a lack of reaction sites on the CA/CS and HO/CS films. In the case of CA, it is likely that the dehydration condensation reaction to generate the reaction sites occurred slower than the Schiff base production and the Michael type addition with CS on the catechol moieties at 30 °C.[39] In contrast, we supposed that the lack of a reaction site on the HO/CS system was due to the lower reactivity of the unconjugated carboxy groups because the carboxy groups in all PHs except for HO became conjugated to styryl or phenyl groups, while those in HO became unconjugated.

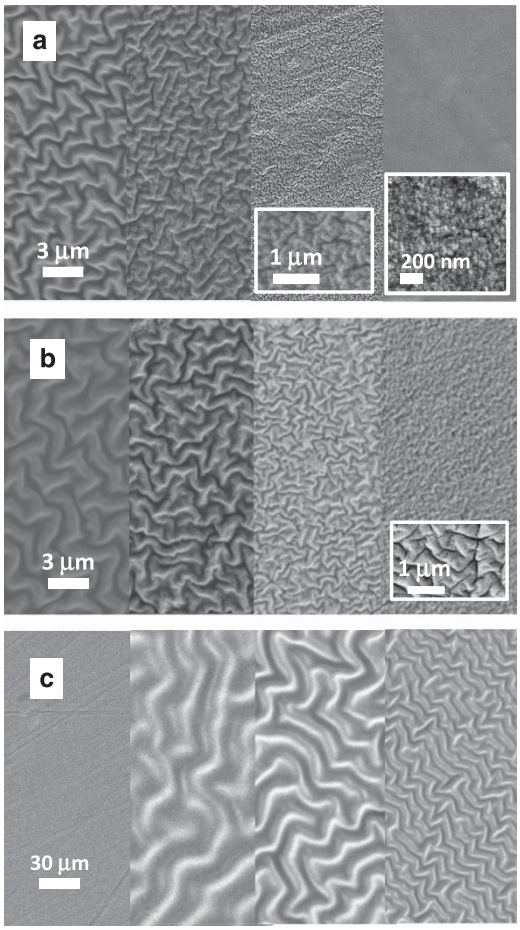

Figure 2 Plane-view SEM images of the films obtained with CO (**a**), FE (**b**) and CA (**c**) using different immersion temperatures (30, 40, 50, 60 °C from left). The figure was reproduced from Izawa *et al.*[35,36]

The differences between the HRP-catalyzed reactions of the styryl-type PHs (CO, FE and CA) and the phenyl-type PHs (VA and HO) provided important insight into the structures of the skin layers. The HRP-catalyzed reaction of the styryl-type PHs generated phenoxide radicals that could resonate with the 5′-position or β-position.[40] The coupling reaction of these radicals provided oligomers.[41] In contrast, the HRP-catalyzed reactions of the phenyl-type PHs provided only dimers.[42–44] Despite this, surprisingly, wrinkling occurred on both the VA and HO, as shown in the above SEM images. The results obtained with VA and HO clearly indicated that a vinyl moiety in the styryl-type PHs was not required to induce surface wrinkling. The elemental analysis provided evidence that the PH/CS films included ca. 30–90 times greater PHs than the covalently bound PHs.[35,37] In such conditions, radical coupling between PH and the covalently bound PH occurred more easily than coupling between two covalently bound PHs. In addition, the covalently bound PH was necessary to form a skin layer that induced surface wrinkling as described above. Thus, ionic crosslinking of the dimeric/oligomeric sidechains was the most likely crosslinking structure, as shown in Figure 4. We observed a critical result proving this speculation.[37] The wrinkles were maintained even after soaking in water for 1 week, whereas they disappeared while soaking in a 100 mM NaOH aqueous solution. This experiment indicated that the skin layers were formed by ionic crosslinking because the crosslinks between the carboxylic acid and primary amine groups became dissociated under alkaline conditions.

We successfully determined the thickness of the skin layer using SEM and time-of-flight secondary ion mass spectrometry analyses of the wrinkled FE/CS films.[37] The topmost layer had a thickness of approximately 120 nm, as observed using SEM cross-section imaging. The time-of-flight secondary ion mass spectrometry spectra of the positively charged secondary ions produced from the wrinkled surface showed characteristic fragment ions from the α,β-unsaturated carboxylic acid groups of the oligomeric FE moieties. The thickness estimated from the depth profiles of the characteristic fragment ions showed good agreement with the thickness of the topmost layer observed from the SEM analysis. These results revealed that the thickness of the skin layer was on the order of submicrons (<200 nm). Note that the thickness of the skin layers produced by the HRP-catalyzed reaction did not depend on the choice of PH or on the conditions of the immersion process because the correlation between the wrinkle sizes and mechanical properties, as described below, indicated that large differences did not exist between the skin

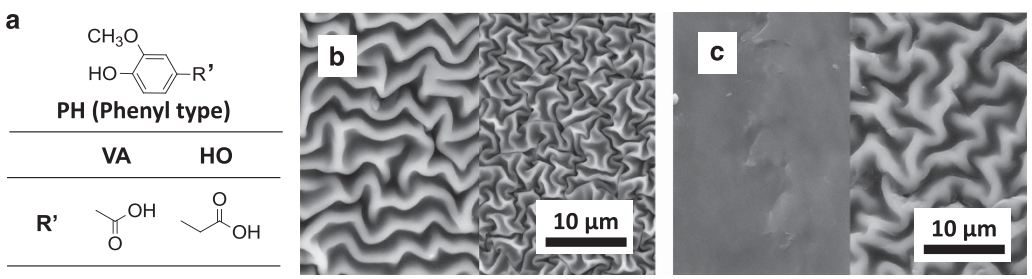

Figure 3 Structures of VA and HO (**a**) and plane-view SEM images of the films obtained with VA (**b**) and HO (**c**) using different immersion temperatures (30, 40 °C from left). The figure was reproduced from Izawa *et al.*[37]

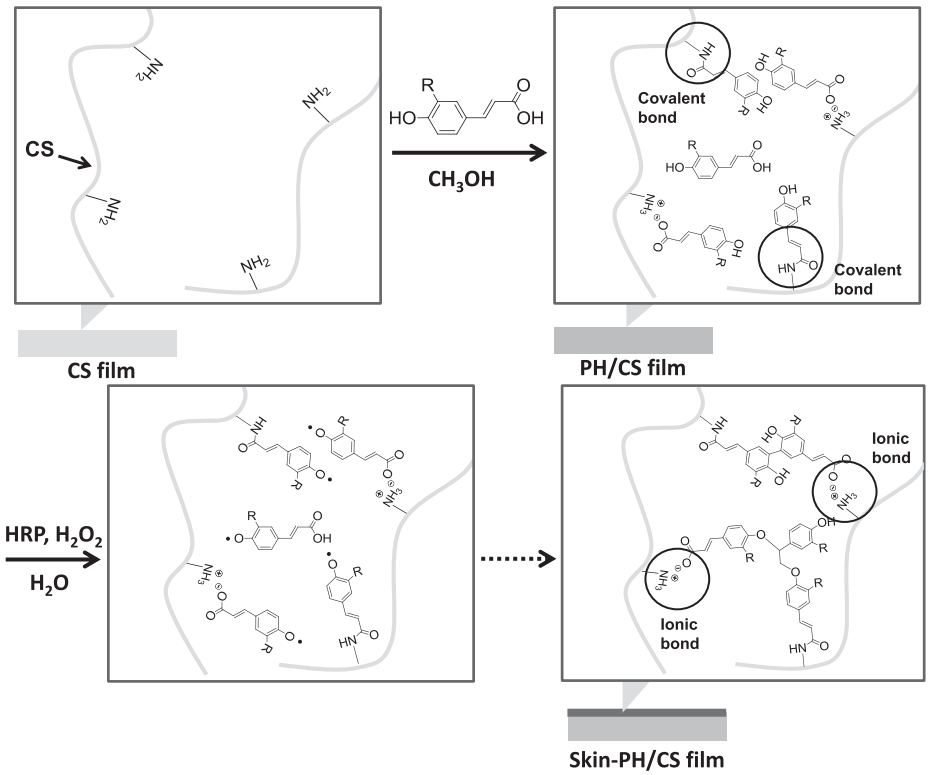

Figure 4 Illustration of the mechanism for the production of the skin layer. The figure was partially reproduced from Izawa *et al.*[37]. A full colour version of this figure is available at the *Polymer Journal* journal online.

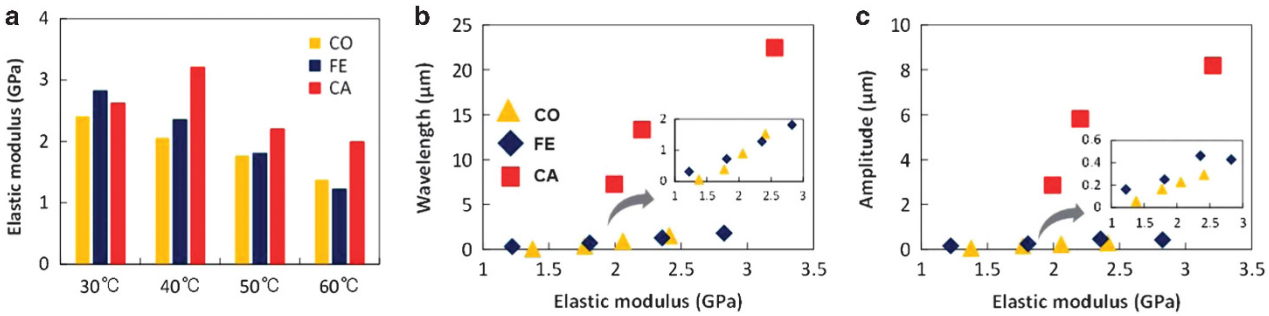

Figure 5 The elastic moduli of the CO/CS, FE/CS, and CA/CS films (**a**) and their correlation with the wrinkle wavelength (**b**) and amplitude (**c**). The figure was reproduced from Izawa *et al.*[36]

thicknesses of the wrinkled films prepared under different immersion conditions.[36]

EFFECTS OF THE MECHANICAL PROPERTIES ON THE WRINKLE MORPHOLOGY

The wrinkle wavelength and amplitude could be controlled by the choice of the PH and immersion temperature. This result implied the occurrence of another phenomenon during the immersion process. In common wrinkled surfaces, the wavelength (λ) of the wrinkles is dependent on the skin thickness (d), and the mechanical properties of the film are described as follows:[12,45]

$$\lambda = 2\pi d\left(\frac{\bar{E}_s}{3\bar{E}_f}\right)^{\frac{1}{3}} \quad (1)$$

where $\bar{E}$ is the plane-strain modulus given by $E/(1-\nu^2)$, the subscripts s and f refer to the skin layer and the foundation (substrate), respectively, E is the elastic modulus, and ν is the Poisson's ratio. In addition, the amplitude (A) of the wrinkles is described as follows:[45]

$$A = d\left(\frac{\varepsilon}{\varepsilon_c} - 1\right)^{\frac{1}{2}} \quad (2)$$

where ε and ε_c are the applied and critical strain, respectively. In addition, ε_c is dependent on $\bar{E}$ as follows:[45]

$$\varepsilon_c = \frac{1}{4}\left(\frac{3\bar{E}_f}{\bar{E}_s}\right)^{\frac{2}{3}} \quad (3)$$

The change in the Poisson's ratio after crosslinking a polymeric material is not large.[46,47] The conditions of the immersion process did not change the thicknesses of the skin layers produced by the HRP-catalyzed reaction because the thickness was determined by the diffusion depth of the HRP relative to the film surface. Thus, the differences between the molecular structures of the PH and the

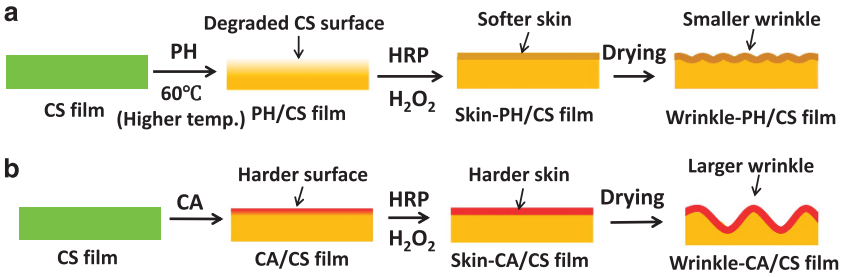

Figure 6 Illustration of mechanisms for the production of smaller wrinkles under treatment at higher immersion temperatures (**a**) and larger wrinkles in the CA/CS system (**b**). The figure was partially reproduced from Izawa *et al.*[36]

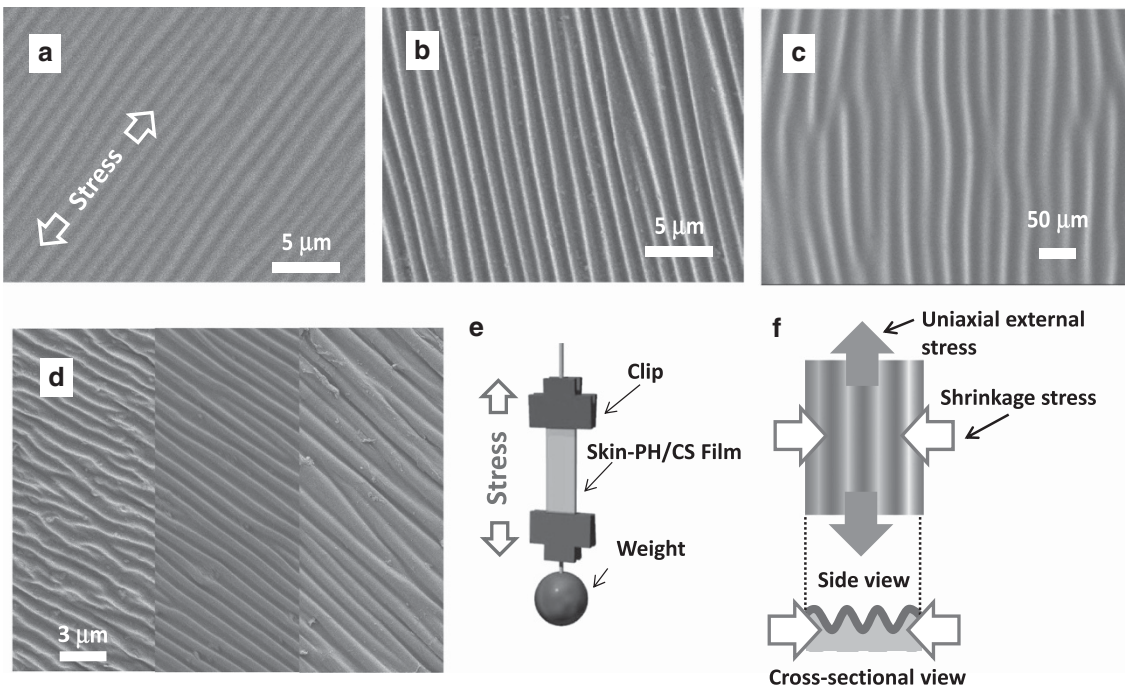

Figure 7 Plane-view SEM images of the wrinkle-CO/CS (**a**), -FE/CS (**b**) and -CA/CS (**c**) films (40 °C immersion) dried under external stress (0.47 MPa) and the wrinkle-CO/CS films (30 °C immersion) dried under external stress (0.19, 0.47, 0.89 MPa from left) (**d**). Illustration of the experiment (**e**) and surface wrinkling under drying stress (**f**). The figure was partially reproduced from Izawa *et al.*[35,36]. A full colour version of this figure is available at the *Polymer Journal* journal online.

immersion temperature should have significantly affected the mechanical properties. To clarify the mechanisms responsible for the different wrinkle sizes, the elastic moduli of the CO/CS, FE/CS and CA/CS films were measured using tensile tests (Figure 5a), in which the elastic moduli of the films gradually decreased with the increase in the immersion temperature.[36] In addition, both the wavelength and amplitude clearly decreased with the decrease in the elastic moduli (Figure 5b–c), indicating that the phenomenon causing the decreased elastic moduli involved decreasing the wrinkle wavelength and amplitude. This result also indicated that there were no large differences in the skin thicknesses among the wrinkled films.

After conducting a gel permeation chromatography analysis, we revealed that the reason for the decreased elastic moduli was the decomposition of CS around the film surface caused by the carboxyl groups during immersion in the PH–methanol solutions. The decomposition was accelerated at higher immersion temperatures, indicating that higher temperatures led to the formation of softer skins, thereby inducing smaller wrinkles (Figure 6a). In contrast, with respect to the larger wrinkles in the CA/CS system, the aforementioned reactivity of the catechol moieties in CA made a harder skin, which in turn caused larger wrinkles (Figure 6b). Hence, we concluded that wrinkle sizes with this system were predominately determined by the hardness of the skin layers. This phenomenon is consistent with the fundamentals of surface wrinkling in nature.[12]

Softer skins generally induce smaller wrinkles, as described in equations (1)–(3). This is consistent with our results. In contrast, the dimple formation shown on the CO/CS system at 60 °C can be explained by the decreased shrinkage stress on the softened skin. The wrinkles observed at high overstress conditions can be described as follows[48]

$$\frac{\sigma}{\sigma_c} \gg 1 \tag{4}$$

where σ and σ_c are the applied and critical stresses, respectively. In contrast, the dimples observed at low overstress conditions can be described as follows:[48]

$$\frac{\sigma}{\sigma_c} \geqslant 1 \tag{5}$$

Here, σ_c is described as follows:[45,48]

$$\sigma_c = \frac{\overline{E}_s}{4}\left(\frac{3\overline{E}_f}{\overline{E}_s}\right)^{\frac{2}{3}} \quad (6)$$

Hence, σ_c is lower on softer skin, as described by equation (6). However, decreasing σ_c does not lead to dimple formation, as described in equations (4) and (5). Therefore, we supposed that the generated shrinkage stress (σ) was decreased as the skin was softened to form the dimples after immersion treatment at 60 °C and that σ/σ_c was predominately determined by σ in this system. Indeed, polysaccharide materials having higher elastic moduli cause stronger aggregation upon drying.[49,50]

The production of larger wrinkles in the VA/CS and HO/CS systems than in the FE/CS system could be explained by the number of ionic bonds.[37] The order of the speculated quantity of ionic bonds from the infrared analysis is as follows: HO/CS system > VA/CS system > FE/CS system; meanwhile, the wrinkle wavelengths and amplitudes decreased in the following order: HO/CS > VA/CS > FE/CS. These relationships indicated that a higher quantity of ionic bonds resulted in a harder skin layer, leading to larger wrinkles.

EFFECT OF EXTERNAL STRESSES ON THE WRINKLE MORPHOLOGY DURING DRYING

The wrinkles formed gradually with time upon water evaporation as shown in Figure 1. On the basis of this observation, we predicted that the morphology of the wrinkles could be controlled by external stresses during drying. Thus, we investigated the effects of applied external stresses. After the skin-CO/CS, FE/CS or CA/CS film was clamped after treatment at 40 °C, a weight was added to one end, and the film was hung for 12 h in air at 40 °C (Figure 7e); the applied external stress by weight was 0.47 MPa. In all cases, anisotropic wrinkles were observed on the films depending on the direction of the applied stress (Figure 7a–c). These results indicated that the generated shrinkage stress was regulated because the uniaxial external stress prevented vertical surface wrinkling (Figure 7f).

We further investigated the effect of the stress magnitude on the wrinkle morphology (Figure 7d).[36] The skin-CO/CS film after treatment at 30 °C was dried under 0.19, 0.47 or 0.89 MPa of external stress. Higher order wrinkles were obtained with the application of 0.47 and 0.89 MPa than with 0.19 MPa. The mean wrinkle wavelengths under 0, 0.19 and 0.47 MPa of drying stress were 1.53 ± 0.19, 1.13 ± 0.11 and 0.90 ± 0.05 μm, respectively, indicating slight decreases with the increasing stress. In contrast, the mean wrinkle amplitudes under 0, 0.19 and 0.47 MPa of drying stress were 0.30 ± 0.03, 0.32 ± 0.05 and 0.35 ± 0.07 μm, respectively, indicating slight increases with the increasing stress. We conjectured that the generated shrinkage stress was increased with the increasing drying stress. In contrast, the mean wrinkle wavelength under 0.89 MPa was increased to 1.25 ± 0.16 μm, but the amplitude was decreased to 0.24 ± 0.03 μm. This result was due to the plastic deformation of the film after applying the larger drying stress because the yield stress of the film was 0.53 MPa. Although the wavelength and amplitude were changed by varying the drying stresses, the degree of variation was small compared to the changes caused by different immersion temperatures, indicating that the wrinkle wavelength and amplitude were predominately determined by the mechanical properties of the films, even under applied drying stresses.

CONCLUSIONS AND OUTLOOK

We have overviewed a novel surface wrinkling system by means of a lignification-mimetic reaction. Microscopic wrinkles were fabricated on the surfaces of CS films using a facile procedure involving immersion, a HRP-catalyzed surface reaction, and drying. We revealed that the immersion process induced surface wrinkling by the formation of covalent bonds between the CS substrate and PH. The PH-bound moieties acted as reaction sites for crosslinking via the HRP-catalyzed reaction and yielded a skin layer on the order of submicrons. The crosslinking structure that was capable of skin formation consisted of ionic bonds composed of CS and dimeric/oligomeric PH residues on the CS. In addition, the wrinkle sizes could be controlled by the choice of temperature during the immersion process because the CS around the film surface was decomposed by the carboxyl groups of the PH. The decomposition was accelerated by applying a higher immersion temperature, and the greater degree of decomposition led to the formation of softer skins. In fact, wrinkle sizes with this system were predominately determined by the hardness of the skin layers. We also revealed that the wrinkle direction was highly controllable by applying moderate levels of external stress. Notably, this is a totally biobased system involving only green materials and processes.

We found that surface wrinkling upon drying is an effective method for fabricating wrinkled materials from CS. The wrinkle morphology could be controlled by precisely controlling the surface hardness and by applying external stresses during drying. Furthermore, we revealed the importance of ionic crosslinking for skin layer formation and inducing surface wrinkling upon drying. These perspectives will enable the development of various wrinkled biomaterials that are applicable as cell culture scaffolds and biological adhesives. Our approach has opened the door for using wrinkled materials in bioengineering.

CONFLICT OF INTEREST

The author declare no conflict of interest.

ACKNOWLEDGEMENTS

This work was supported in part by JSPS KAKENHI Grant Number 16K05916. The author sincerely acknowledges Prof Hiroyuki Saimoto, Prof Shinsuke Ifuku, Prof Minoru Morimoto, Noriko Okuda, Arisu Moriyama, Yuka Miyazaki, and Yuki Dote at Tottori University and Prof Orlando J Rojas at Aalto University for their contributions to this study.

1 Bhushan, B. Biomimetics: lessons from nature—an overview. *Philos T R Soc A* **367**, 1445–1486 (2009).
2 Bhushan, B. & Jung, Y. C. Natural and biomimetic artificial surfaces for superhydrophobicity, self-cleaning, low adhesion, and drag reduction. *Prog Mater Sci* **56**, 1–108 (2011).
3 Ruiz-Hitzky, E., Darder, M., Aranda, P. & Ariga, K. Advances in biomimetic and nanostructured biohybrid materials. *Adv Mater* **22**, 323–336 (2010).
4 Ishihara, K. Highly lubricated polymer interfaces for advanced artificial hip joints through biomimetic design. *Polym J* **47**, 585–597 (2015).
5 Takeoka, Y. Angle-independent colored materials based on the Christiansen effect using phase-separated polymer membranes. *Polym J* **49**, 301–308 (2017).
6 Kawamura, A., Kohri, M., Morimoto, G., Nannichi, Y., Taniguchi, T. & Kishikawa, K. Full-color biomimetic photonic materials with iridescent and non-iridescent structural colors. *Sci Rep-Uk* **6**, 33984 (2016).
7 Otsuka, T., Fujikawa, S., Yamane, H. & Kobayashi, S. Green polymer chemistry: the biomimetic oxidative polymerization of cardanol for a synthetic approach to 'artificial urushi'. *Polym J* **49**, 335–343 (2017).
8 Pandian, G. N. & Sugiyama, H. Nature-inspired design of smart biomaterials using the chemical biology of nucleic acids. *Bull Chem Soc Jpn* **89**, 843–868 (2016).
9 Kawamura, A., Kohri, M., Yoshioka, S., Taniguchi, T. & Kishikawa, K. Structural color tuning: mixing melanin-like particles with different diameters to create neutral colors. *Langmuir* **33**, 3824–3830 (2017).

10 Park, S. Y., Hwang, I. S., Lee, H. J. & Song, C. E. Biomimetic catalytic transformation of toxic alpha-oxoaldehydes to high-value chiral alpha-hydroxythioesters using artificial glyoxalase I. *Nat Commun* **8**, 14877 (2017).
11 Shao, Y., Taniguchi, K., Gurdziel, K., Townshend, R. F., Xue, X., KMA, Yong, Sang, J., Spence, J. R., Gumucio, D. L. & Fu, J. Self-organized amniogenesis by human pluripotent stem cells in a biomimetic implantation-like niche. *Nat Mater* **16**, 419 (2017).
12 Genzer, J. & Groenewold, J. Soft matter with hard skin: from skin wrinkles to templating and material characterization. *Soft Matter* **2**, 310–323 (2006).
13 Ionov, L. Biomimetic 3D self-assembling biomicroconstructs by spontaneous deformation of thin polymer films. *J Mater Chem* **22**, 19366–19375 (2012).
14 Chen, C. M. & Yang, S. Wrinkling instabilities in polymer films and their applications. *Polym Int* **61**, 1041–1047 (2012).
15 Ohzono, T., Suzuki, K., Yamaguchi, T. & Fukuda, N. Tunable optical diffuser based on deformable wrinkles. *Adv Opt Mater* **1**, 374–380 (2013).
16 Lee, S. G., Kim, H., Choi, H. H., Bong, H., Park, Y. D., Lee, W. H. & Cho, K. Evaporation-induced self-alignment and transfer of semiconductor nanowires by wrinkled elastomeric templates. *Adv Mater* **25**, 2162–2166 (2013).
17 Stenberg, H., Matikainen, A., Daniel, S., Nuutinen, T., Stenberg, P., Honkanen, S., Pakkanen, T., Vahimaa, P. & Suvanto, M. Self-organized Polymer Wrinkles: a lithography-free pathway for surface-enhanced raman scattering (SERS) substrates. *Macromol Mater Eng* **300**, 386–390 (2015).
18 Li, Y. Y., Dai, S. X., John, J. & Carter, K. R. Superhydrophobic surfaces from hierarchically structured wrinkled polymers. *Acs Appl Mater Inter* **5**, 11066–11073 (2013).
19 Davis, C. S., Martina, D., Creton, C., Lindner, A. & Crosby, A. J. Enhanced adhesion of elastic materials to small-scale wrinkles. *Langmuir* **28**, 14899–14908 (2012).
20 Zhao, Z. Q., Gu, J., Zhao, Y., Guan, Y., Zhu, X. X. & Zhang, Y. Hydrogel thin film with wwelling-induced wrinkling patterns for high-throughput generation of multicellular spheroids. *Biomacromolecules* **15**, 3306–3312 (2014).
21 Bowden, N., Brittain, S., Evans, A. G., Hutchinson, J. W. & Whitesides, G. M. Spontaneous formation of ordered structures in thin films of metals supported on an elastomeric polymer. *Nature* **393**, 146–149 (1998).
22 Gu, J. J., Li, X. Y., Ma, H. C., Guan, Y. & Zhang, Y. J. One-step synthesis of PHEMA hydrogel films capable of generating highly ordered wrinkling patterns. *Polymer* **110**, 114–123 (2017).
23 Efimenko, K., Rackaitis, M., Manias, E., Vaziri, A., Mahadevan, L. & Genzer, J. Nested self-similar wrinkling patterns in skins. *Nat Mater* **4**, 293–297 (2005).
24 Endo, H., Mochizuki, Y., Tamura, M. & Kawai, T. Fabrication and functionalization of periodically aligned metallic nanocup arrays using colloidal lithography with a sinusoidally wrinkled substrate. *Langmuir* **29**, 15058–15064 (2013).
25 Barel, A. O., Paye, M. & Maibach, H. *Handbook of Cosmetic Science and Technology* 2nd edn 91–106 (CRC Press, 2009).
26 Imokawa, G. & Takema, Y. Fine wrinkle formation. Etiology and prevention. *Cosmet Toilet* **108**, 65–77 (1993).
27 Tsukahara, K., Hotta, M., Fujimura, T., Haketa, K. & Kitahara, T. Effect of room humidity on the formation of fine wrinkles in the facial skin of Japanese. *Skin Res Technol* **13**, 184–188 (2007).
28 Huraux, K., Narita, T., Bresson, B., Fretigny, C. & Lequeux, F. Wrinkling of a nanometric glassy skin/crust induced by drying in poly(vinyl alcohol) gels. *Soft Matter* **8**, 8075–8081 (2012).
29 Rizzieri, R., Mahadevan, L., Vaziri, A. & Donald, A. Superficial wrinkles in stretched, drying gelatin films. *Langmuir* **22**, 3622–3626 (2006).
30 Zhu, H. L., Luo, W., Ciesielski, P. N., Fang, Z., Zhu, J. Y., Henriksson, G., Himmel, M. E. & Hu, L. Wood-derived materials for green electronics, biological devices, and energy applications. *Chem Rev* **116**, 9305–9374 (2016).
31 Zhu, H. L., Luo, W., Ciesielski, P. N., Fang, Z., Zhu, J. Y., Henriksson, G., Himmel, M. E. & Hu, L. Correction To Wood-derived materials for green electronics, biological devices, and energy applications. *Chem Rev* **116**, 12650–12650 (2016).
32 Doherty, W. O. S., Mousavioun, P. & Fellows, C. M. Value-adding to cellulosic ethanol: Lignin polymers. *Ind Crop Prod* **33**, 259–276 (2011).
33 Barcelo, A. R. Lignification in plant cell walls. *Int Rev Cytol* **176**, 87–132 (1997).
34 Veitch, N. C. Horseradish peroxidase: a modern view of a classic enzyme. *Phytochemistry* **65**, 249–259 (2004).
35 Izawa, H., Okuda, N., Ifuku, S., Morimoto, M., Saimoto, H. & Rojas, O. J. Bio-based wrinkled surfaces harnessed from biological design principles of wood and peroxidase activity. *ChemSusChem* **8**, 3892–3896 (2015).
36 Izawa, H., Okuda, N., Ifuku, S., Morimoto, M., Saimoto, H. & Rojas, O. J. Biobased wrinkled surfaces induced by wood mimetic skins upon drying: effect of mechanical properties on wrinkle morphology. *Langmuir* **32**, 12799–12804 (2016).
37 Izawa, H., Dote, Y., Okuda, N., Sumita, M., Ifuku, S., Morimoto, M. & Saimoto, H. Wood-mimetic skins prepared using horseradish peroxidase catalysis to induce surface wrinkling of chitosan film upon drying. *Carbohydr Polym* **173**, 519–525 (2017).
38 Basavaprabhu, Muniyappa, K., Panguluri, N. R., Veladi, P. & Sureshbabu, V. V. A simple and greener approach for the amide bond formation employing $FeCl_3$ as a catalyst. *New J Chem* **39**, 7746–7749 (2015).
39 Gray, K. M., Kim, E., Wu, L., Liu, Y., Bentley, W. E. & Payne, G. F. Biomimetic fabrication of information-rich phenolic-chitosan films. *Soft Matter* **7**, 9601–9615 (2011).
40 Oudgenoeg, G., Dirksen, E., Ingemann, S., Hilhorst, R., Gruppen, H., Boeriu, C. G., Piersma, S. R., van Berkel, W. J., Laane, C. & Voragen, A. G. Horseradish peroxidase-catalyzed oligomerization of ferulic acid on a template of a tyrosine-containing tripeptide. *J Biol Chem* **277**, 21332–21340 (2002).
41 Izawa, H., Miyazaki, Y., Ifuku, S., Morimoto, M. & Saimoto, H. Fully biobased oligophenolic nanoparticle prepared by horseradish peroxidase-catalyzed polymerization. *Chem Lett* **45**, 631–633 (2016).
42 Ci, Y. X. & Wang, F. Catalytic effects of peroxidase-like metalloporphyrins on the fluorescence reaction of homovanillic-acid with hydrogen-peroxide. *Fresen J Anal Chem* **339**, 46–49 (1991).
43 Foppoli, C., Coccia, R., Blarzino, C. & Rosei, M. A. Formation of homovanillic acid dimer by enzymatic or Fenton system—catalyzed oxidation. *Int J Biochem Cell Biol* **32**, 657–663 (2000).
44 Tai, A., Sawano, T. & Ito, H. Antioxidative properties of vanillic acid esters in multiple antioxidant assays. *Biosci Biotech Bioch* **76**, 314–318 (2012).
45 Chung, J. Y., Nolte, A. J. & Stafford, C. M. Surface wrinkling: a versatile platform for measuring thin-film properties. *Adv Mater* **23**, 349–368 (2011).
46 Amsden, B. G., Sukarto, A., Knight, D. K. & Shapka, S. N. Methacrylated glycol chitosan as a photopolymerizable biomaterial. *Biomacromolecules* **8**, 3758–3766 (2007).
47 Greaves, G. N., Greer, A. L., Lakes, R. S. & Rouxel, T. Poisson's ratio and modern materials. *Nat Mater* **10**, 823–837 (2011).
48 Breid, D. & Crosby, A. J. Effect of stress state on wrinkle morphology. *Soft Matter* **7**, 4490–4496 (2011).
49 Izawa, H., Nawaji, M., Kaneko, Y. & Kadokawa, J. Preparation of glycogen-based polysaccharide materials by phosphorylase-catalyzed chain elongation of glycogen. *Macromol Biosci* **9**, 1098–1104 (2009).
50 Suchy, M., Kontturi, E. & Vuorinen, T. Impact of drying on wood ultrastructure: similarities in cell wall alteration between native wood and isolated wood-based fibers. *Biomacromolecules* **11**, 2161–2168 (2010).

Hironori Izawa is an assistant professor at Tottori University. He received his MS degree in 2005 from Tohoku University and his PhD in 2010 from Kagoshima University under Prof. Shin-ichiro Shoda and Prof. Jun-ichi Kadokawa, respectively. He spent postdoctoral research periods at the National Institute for Materials Science (NIMS) under the supervision of Prof. Katsuhiko Ariga (2010–2012), and moved to Tottori University in 2012. His major interests are the preparation of functional polysaccharide materials, including gel and film materials, with enzymatic or chemical processes. He received the Award for Encouragement of Research in Polymer Science from the Society of Polymer Science, Japan (2016).